Adaptive Fourier Analysis in the Case of Data Loss

András Palkó
Department of Measurement and Information Systems
Budapest University of Technology and Economics
Budapest, Hungary
palko@mit.bme.hu

László Sujbert
Department of Measurement and Information Systems
Budapest University of Technology and Economics
Budapest, Hungary
sujbert@mit.bme.hu

***Abstract*—The Adaptive Fourier Analyzer has been developed for measuring the harmonic components of periodic signals with changing or unknown fundamental frequency. Vibration analysis of rotating machines, active noise control or harmonic component measurements of the lines are typical applications. Nowadays, radio or Internet-based communication is gaining popularity in various fields, e.g., in signal processing. Due to the not reliable real-time communication, some of the data are lost during the transmission.**

In this paper, an extension of the Adaptive Fourier Analyzer is presented which is able to handle data loss. The paper briefly presents the mathematical description of the data loss and the modification of the Resonator-Based Observer for data loss. The novelty of this paper is the modification of the Adaptive Fourier Analyzer for signals with missing samples. The performance of the algorithm is demonstrated with simulation and measurement examples.

***Index Terms*—Adaptive Fourier analysis, data loss, digital signal processing, order tracking**

I. Introduction

In many applications periodic signals with unknown or changing fundamental frequency are to be measured. A typical task is to determine their harmonic components, which is called order tracking [1]. Some examples are vibration analysis of rotating machines, active noise control or measurement of the harmonic components of the line voltages.

An observer-based approach can be utilized to solve the problem. For a constant and known fundamental frequency, this yields the Resonator-Based Observer (RBO) [2]. When the fundamental frequency is unknown or changes, it can be estimated based on the fundamental component. This is the idea behind the Adaptive Fourier Analyzer (AFA) [3], [4].

The AFA has two main outputs. On one hand, it is able to estimate the fundamental frequency of a periodic signal in a wide range. On the other hand, it is a spectral estimator: it performs harmonic decomposition based on the frequency estimate. Consequently, when the structure has converged, the exact values of the Fourier coefficients are available.

Despite being a nonlinear observer, many simulations, measurement experiences and practical applications showed its robust, stable behavior. According to the experiences, the AFA is stable even in the presence of frequency jumps, varying upper harmonics and noise. It must be noted that the algorithm is not sensitive to the numerical problems arising from limited word length.

Based on the original algorithm, a family of adaptive Fourier analyzers were developed. [5] presented a modification able to track linear, logarithmic or hyperbolic frequency sweep. [6] and [7] gave modifications with increased robustness and noise rejection. [8] separated the frequency and the Fourier component updates to two alternating stages, resulting in the Block AFA algorithm. Although the convergence of the original algorithm is not yet proved, exact conditions can be derived for the Block AFA.

With decreasing the fundamental frequency, the AFA will have higher computation requirements. However, the signal will be significantly oversampled. In [9] a decimating filter bank is applied to keep the computational demand in hand. [10] and [11] also present solutions with reduced complexity.

Nowadays, with the spreading of sensor networks, radio or Internet-based communication is gaining popularity in various applications. Due to the not reliable protocols and equipment, the message can be partially damaged during the transmission, the measurement can be hindered by external circumstances. As a result, some samples may be missing or invalid.

In this paper, we present the extension of the AFA for the case of missing samples. The RBO has been previously extended to handle data loss [12]. As the original AFA uses the original RBO, the proposed structure uses the RBO extended for data loss. The performance of the proposed structure is demonstrated with simulations and measurements.

The paper is arranged as follows: Section II summarizes the original RBO and AFA structures, and gives the used mathematical description of the data loss. Section III deals with the modifications of the RBO and the AFA for the case of data loss. The performance of the proposed structure is demonstrated with simulation and measurement examples in Section IV. The paper concludes in Section V.

II. Preliminaries

A. Resonator-Based Observer

1) Conceptual Signal Model: The conceptual signal model plays a central role in the RBO. Generally, a periodic signal

The project was funded by the European Union, co-financed by the European Social Fund (EFOP-3.6.2-16-2017-00013). The research reported in this paper and carried out at the BME has been supported by the NRDI Fund based on the charter of bolster issued by the NRDI Office under the auspices of the Ministry for Innovation and Technology.

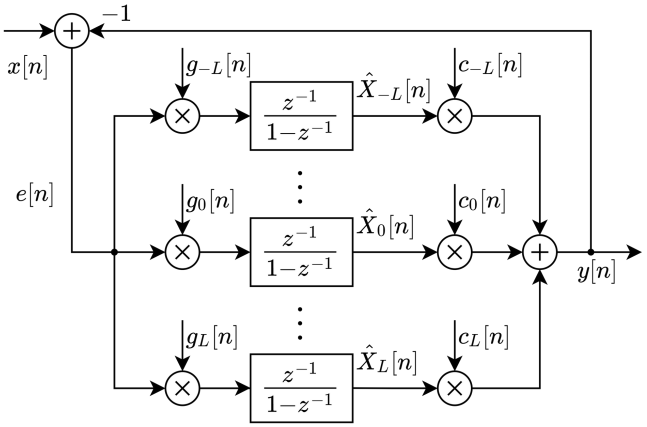

Fig. 1. Block diagram of the RBO

can be described with its complex Fourier series:

$$x[n] = \sum_{k=-L}^{L} X_k c_k[n] \tag{1}$$

where X_k is the kth Fourier coefficient and $c_k[n]$ is a complex exponential:

$$c_k[n] = \mathrm{e}^{\mathrm{j}2\pi f_1 kn} \quad (k = -L, \ldots, L) \tag{2}$$

where j is the imaginary unit and f_1 is the fundamental frequency of $x[n]$ (relative to the sampling frequency).

Assuming proper anti-aliasing filter, the following holds:

$$Lf_1 < 0.5 < (L+1)f_1 \tag{3}$$

Note that there is no component modeled at the Nyquist frequency. This is not a problem for real signals.

2) Observer: Based on the conceptual signal model, the corresponding observer can be designed. As the Fourier coefficients are the state variables of the signal model, the observer will estimate them directly. With the $\hat{X}_k$ estimated Fourier coefficients the estimate of the input signal can be calculated:

$$y[n] = \sum_{k=-L}^{L} \hat{X}_k c_k[n] \tag{4}$$

The estimation error is

$$e[n] = y[n] - x[n] \tag{5}$$

The update equation of the observer is

$$\hat{X}_k[n+1] = \hat{X}_k[n] + g_k[n]e[n] \tag{6}$$

where $g_k[n]$ is a reciprocal complex exponential:

$$g_k[n] = \frac{1}{N}\bar{c}_k[n] = \frac{1}{N}\mathrm{e}^{-\mathrm{j}2\pi f_1 kn} \quad (k = -L, \ldots, L) \tag{7}$$

where $\bar{\cdot}$ denotes the complex conjugate and $N = 2L+1$ is the number of components. The observer is depicted in Fig. 1.

In steady-state, the estimated and the original Fourier-coefficients are equal, thus the signal is perfectly reconstructed [2]. Although the steady-state is reached in infinite steps, when (3) holds, the settling is fast.

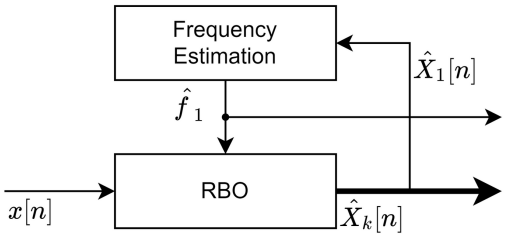

Fig. 2. Block diagram of the AFA

The observer provides the unbiased estimates of the Fourier coefficients of the input signal, its only requirement is that the fundamental frequency has to be known.

B. Adaptive Fourier Analyzer

1) Fundamental Frequency Estimation: The adaptive Fourier analyzer tries to estimate the value of the fundamental frequency instead of requiring its knowledge. It can be observed, that $\hat{X}_1[n]$ rotates approximately proportionally with the fundamental frequency error [4]. Using this, the frequency estimator can be updated as

$$f_1[n+1] = f_1[n] + G \cdot \mathrm{angle}(\hat{X}_1[n+1], \hat{X}_1[n]) \tag{8}$$

where the $\mathrm{angle}(\cdot,\cdot)$ function returns the angle between two complex numbers. The gain G controls the speed of the frequency adaptation. Because of the approximate nature of (8) and the noises, the gain G is chosen as $G = \frac{1}{2\pi N}$ [3].

It can be seen that the frequency estimator is updated on the new and old values of the state variable $\hat{X}_1$.

2) Algorithm: The block diagram of the AFA can be seen in Fig. 2. An RBO estimates the harmonic components, and the fundamental frequency is estimated from the fundamental component. Here only the steps of the algorithm are presented, for detailed explanations see [4].

The steps of the algorithm are the following:

Initialization: the $L[0]$ initial number of components is arbitrary.

$$N[0] = 2L[0] + 1, \quad f_1[0] = \frac{1}{N[0]} \tag{9}$$

$$\hat{X}_k[0] = 0, \quad c_k[0] = 1, \quad g_k[0] = 1 \tag{10}$$

for $k = -L[0], \ldots, L[0]$.

Operation: for each sample

1) Calculate the $y[n]$ output like in (4).
2) Determine the $e[n]$ error by (5).
3) Update the $\hat{X}_k[n+1]$ Fourier coefficients using (6).
4) Update the $f_1[n+1]$ fundamental frequency by (8).
5) Constrain the $f_1[n+1]$ fundamental frequency into the range $[f_{\min}, f_{\max}]$. The maximal relative fundamental frequency is just below $1/3$ (see step 7). As the fundamental frequency decreases, the number of modeled components grow. To limit the computation time, a positive minimal fundamental frequency can be set.
6) Rotate the complex exponentials c_k and g_k:

$$c_k[n+1] = c_k[n]\mathrm{e}^{\mathrm{j}2\pi f_1[n+1]k} \tag{11}$$

$$g_k[n+1] = \frac{1}{N}\bar{c}_k[n+1] \tag{12}$$

for $k = -L[n], \ldots, L[n]$. Such an update makes the phase transition continuous.

7) As f_1 can significantly differ from its initial value during operation, $L[n]$ should be changed accordingly:

$$\begin{aligned} L[n+1]f_1[n+1] &< 0.5 - \frac{1}{2N[n]} \\ 0.5 - \frac{1}{2N[n]} &< (L[n+1]+1)f_1[n+1] \end{aligned} \tag{13}$$

and of course $N[n+1] = 2L[n+1]+1$ is updated as well.

8) If $L[n+1] < L[n]$, then the components with order over $L[n+1]$ are canceled.
If $L[n+1] > L[n]$, then new components are started with the following initialization:

$$\hat{X}_k[0] = 0, \quad c_k[0] = 1, \quad g_k[0] = 1 \tag{14}$$

C. Data Loss

1) Basic Definitions: Data loss can be described in discrete time with a so-called $K[n]$ availability indicator function:

$$K[n] = \begin{cases} 1 & \text{if the sample is available at } n \\ 0 & \text{if the sample is lost at } n \end{cases} \tag{15}$$

This indicator function is assumed to be known. The data availability rate μ can be defined as

$$\mu = \mathbb{P}\left(K[n] = 1\right) \tag{16}$$

where $\mathbb{P}(\cdot)$ is the probability operator.

A signal $x[n]$ subject to data loss can be modeled as a product:

$$x[n] = K[n]x_0[n] \tag{17}$$

where $x_0[n]$ is the original signal.

The data loss is block-based when the data are grouped into fixed size blocks, and these blocks are either fully available or fully lost.

2) Data Loss Models: There exists a variety of data loss models. Here only the models used in our simulations are introduced, for a more detailed description we refer to [12], [13].

a) Random Independent Model: The random independent model is the simplest data loss model. It has a single parameter (μ), which is the probability of getting an available sample at any time step. The availability of the different samples is independent of each other, this model has no memory.

b) Two-State Markov Model: The availability of the samples in the two-state Markov model forms a two-state Markov chain. This model has two parameters: the probability of getting a lost sample after an available one (p), and getting an available sample after a lost one (q).

The data availability rate of the two-state Markov model can be calculated as

$$\mu = \frac{q}{p+q} \tag{18}$$

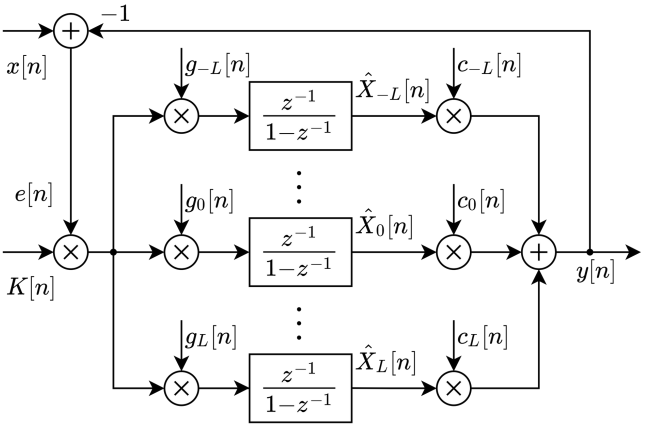

Fig. 3. Block diagram of the RBO in the case of data loss

c) Periodic Data Loss: The data loss is periodic, when the indicator function is periodic: $K[n] = K[n+P]$ for all n, and $P > 0$ is its period when it is the smallest such P.

A periodic data loss is synchronized if the original signal is periodic and the two periods are equal. This means that the missing samples are at the same place in each period.

III. Adaptive Fourier Analyzer in the Case of Data Loss

In the case of data loss, there are some modifications to the RBO and AFA structures.

A. Resonator-Based Observer in the Case of Data Loss

Modeling the data loss as in (17), the conceptual signal model gets an extra term:

$$x[n] = K[n] \sum_{k=-L}^{L} X_k c_k[n] \tag{19}$$

Even if the input signal is subject to data loss, the observer continues to estimate the Fourier coefficients of the original signal. In steady state, the original signal is reconstructed perfectly, without using the lost samples.

For lost samples, the estimation error should be treated as zero, since there is no new measurement to update the estimates with. This can be done by multiplying the error with the indicator function. The update equation of the observer becomes

$$\hat{X}_k[n+1] = \hat{X}_k[n] + g_k[n]K[n]e[n] \tag{20}$$

The corresponding observer is depicted in Fig. 3.

When data loss occurs, the convergence becomes more complicated. Exact results are available for the sufficient and necessary conditions of the convergence of the Fourier coefficients for the RBO at a constant frequency [12]. As an example, the harmonic coefficient estimates are biased if the data loss is synchronized. In practice, this case can happen e.g. when an AD-converter is overdriven by a periodic signal. However, it is conceivable that even if the harmonic component estimates are biased, the frequency can be estimated accurately.

B. Adaptive Fourier Analyzer in the Case of Data Loss

Let us consider signals with lost samples. While the samples are available, frequency estimation can be done by (8). When we reach a lost sample, $\hat{X}_1$ is not changed, so there is no frequency update (there should not be, because there is no new information).

Assuming a sinusoidal signal and inaccurate frequency estimate, P consecutively lost samples would result in $P+1$ times greater angle between $\hat{X}_1[n+1]$ and $\hat{X}_1[n]$ in steady state. Thus the frequency estimation formula can be modified to

$$f_1[n+1] = f_1[n] + \frac{G}{P[n]+1} \cdot \mathrm{angle}(\hat{X}_1[n+1], \hat{X}_1[n]) \quad (21)$$

where $P[n]$ is the number of consecutive lost samples before the actual one.

There are a few modifications to the algorithm also. At the initialization,

$$P[0] = 0 \quad (22)$$

is set.

During operation, (20) is used instead of (6) for the state update. The fundamental frequency is updated with (21) instead of (8). Finally, after adjusting the number of modeled components, the length of the lost sequence before the current sample is updated:

$$P[n+1] = \begin{cases} P[n]+1 & \text{if } K[n] = 0 \\ 0 & \text{if } K[n] = 1 \end{cases} \quad (23)$$

IV. Examples

A. Illustrative Example

An example is shown in Fig. 4 to illustrate the performance of the proposed structure. A 105 Hz square wave was selected for the input signal, the sampling frequency was 10 kHz. At $n = 500$ a frequency jump occurs to 130 Hz. There is additive white Gaussian noise on the signal with SNR $= 60$ dB. For $n \leq 500$, all samples are available, after that a random independent data loss was applied with $\mu = 80\%$.

The availability was drawn in the top plot using the transformation $0.5K[n] - 2$ to place it under the signals. Its high (low) level still means available (lost) samples. The estimated signal is able to follow the original one: even in the presence of data loss, the estimates converge. The convergence is slower when data loss occurs.

B. Convergence with Random Data Loss

We have tested the proposed structure with numerous simulations in a setup similar to the illustrative example. Noisy (SNR $= 40$ dB) and noiseless sine, triangle and square waves were investigated with frequency jump. The signals were generated by their truncated Fourier series, only the components below the Nyquist frequency were kept. Random independent and two-state Markov data loss models were used with $40\% \leq \mu \leq 100\%$ and block sizes from 1 to 100. General conclusions gained from these simulations are presented in the following.

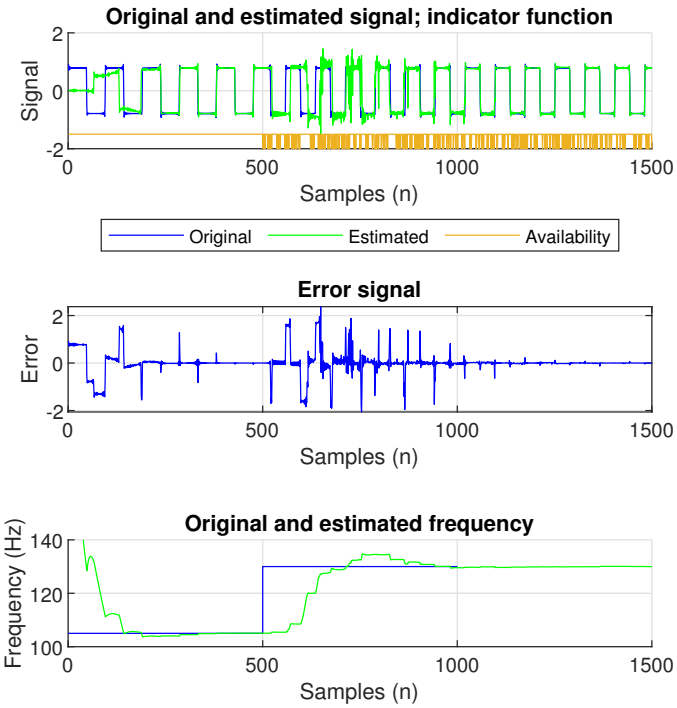

Fig. 4. Illustrative example with random independent data loss ($\mu = 80\%$). Top plot: original input signal without data loss (blue line), $y[n]$ signal estimated by the AFA (green line) and data availability (orange line). Middle plot: $e[n]$ error signal of the AFA. Bottom plot: frequency of the input signal (blue line) and frequency estimated by the AFA (green line).

All three signal shapes produced similar results. As an example, Fig. 5 depicts the convergence of the frequency estimate and the $e[n]$ error signal with an SNR $= 40$ dB triangle wave at different data availability values. The frequency of the input signal jumps from 150 to 180 Hz at $n = 0$. The sampling frequency is again 10 kHz. It is clear that both the frequency and the harmonic components converge, even when only 40% of the data are available. When the number of lost samples is greater, the estimates need more time to settle.

To numerically assess the speed of the convergence, different settling metrics were calculated. The 5% frequency settling index $n_{f,5\%}$ was obtained by the following definition:

$$n_{f,5\%} = \min\{n | f_1[m] \in [f_L, f_U] \ \forall m \geq n\} \quad (24)$$

$$f_{U,L} = (1+\delta) f_0 \pm 0.05|\delta| f_0 \quad (25)$$

where f_0 and $(1+\delta)f_0$ are frequencies before and after the frequency jump. The required number of periods is $N_{f,5\%} = n_{f,5\%}(1+\delta)f_0$.

For the error signal, similar $n_{e,5\%}$ and $N_{e,5\%}$ values were determined. Here the 5% settling means that the error signal stays within the $\pm 5\%$ range of the RMS value of the original signal.

Table I shows the above mentioned convergence metrics averaged from 100 repetitions of the simulation depicted in Fig. 5. The upper half corresponds to the frequency estimates, the lower one to the error signals. The error signals reach their steady state just after the frequency estimates have settled. This is as expected: the settling of the error signal means that the

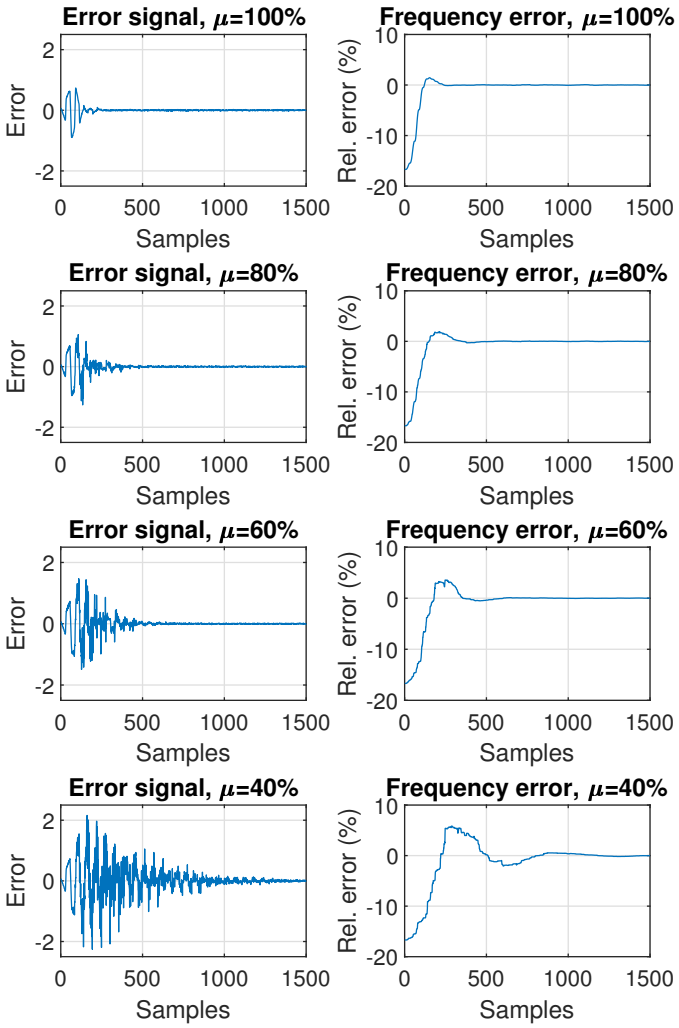

Fig. 5. Convergence with random data loss. Left side: $e[n]$ error signal of the AFA, right side: relative error of the frequency estimation. Each row belongs to an investigated data availability value.

observer creates the same signal as its input, therefore their frequencies are equal.

One could intuitively expect that if e.g. 10% of the samples are missing, the convergence is 10% slower. At μ data availability it would mean $\frac{1}{\mu}$ times larger convergence metrics. However, even the RBO requires more time to settle if there are missing samples. E.g. when the sampling is coherent and a single, randomly selected sample is missing from the first period, in average the settling takes 150% time compared to the case when all samples are available. The settling of the AFA is slightly slower, as the frequency and the harmonic component estimates are coupled.

Considering the rows showing the number of periods required for the settling (capital N values), 20 periods with data loss were enough in average, even at $\mu = 40\%$. Even $\mu = 80\%$ can be considered a strong data loss, and in this case the estimates settled in about twice the time as without data loss.

TABLE I
REQUIRED NUMBER OF SAMPLES AND PERIODS FOR THE FREQUENCY ESTIMATE AND THE ERROR SIGNAL TO CONVERGE AT DIFFERENT DATA AVAILABILITY VALUES

μ	100%	80%	60%	40%
$n_{f,5\%}$	183	266	381	639
$N_{f,5\%}$	3.294	4.784	6.859	11.50
$n_{e,5\%}$	232	374	577	1013
$N_{e,5\%}$	4.176	6.734	10.38	18.24

C. Convergence with Periodic Data Loss

To investigate the influence of periodic data loss, similar simulations were conducted to those in [12]. A 50 Hz periodic signal was sampled at 10 kHz, the amplitudes of the components were inversely proportional to their order ($|X_k| = \frac{1}{k}$, $k = 1, 2, \dots$) and their initial phases were random. Additive white Gaussian noise with $\mathrm{SNR} = 20$ dB was applied.

In these simulations a special kind of periodic data loss was used, where each period consisted of a available samples followed by l lost ones:

$$\begin{aligned} K[1] = \dots = K[a] = 1 \\ K[a+1] = \dots = K[a+l] = 0 \\ K[n] = K[n+a+l] \end{aligned} \tag{26}$$

This will be marked as $P_{a,l}$ data loss.

Fig. 6 shows some selected simulation examples with periodic data loss. The error signals and the frequency errors are shown like in Fig. 5 for three different periodic data loss patterns. Generally, the data loss tolerance is heavily influenced by the relation of the periods of the original signal and the indicator function: the smaller the value of the least common multiple of the periods (compared to the signal period), the less lost samples are tolerated.

The top plots illustrate the convergence with $P_{195,5}$ data loss. Note that $a + l = 200$, so this is a synchronized data loss. On one hand, it is clear that the Fourier coefficients are biased: in steady-state the $e[n]$ error signal shows not only the noise, but it contains a spike at every 200 samples. These spikes mark the places of the lost samples. On the other hand, the frequency is estimated correctly: at $n > 600$ the frequency estimation can be considered accurate.

The middle plots belong to $P_{140,60}$ data loss. The data loss is still synchronized, and now less samples are available in each period. As a result, now even the frequency cannot converge.

The bottom plots were created with $P_{107,60}$ data loss. The data availability is even lower than in the previous case ($\mu = 64.1\%$), but the data loss is no longer synchronized. In fact, the greatest common divisor of the signal and the data loss period lengths is one. Both the frequency and the Fourier coefficient estimates settle.

D. Experimental Results

Measurements were carried out with a test system introduced in [14]. In the test system, wireless sensors perform real-time data acquisition, and these data are transmitted through a gateway node to a PC for processing. In this measurement

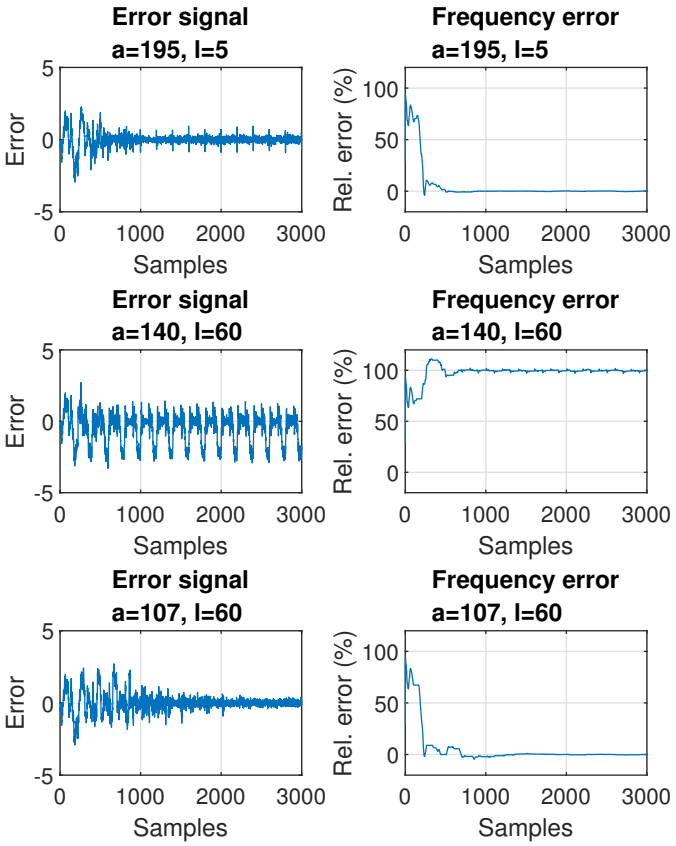

Fig. 6. Convergence of the frequency with periodic data loss. Left side: $e[n]$ error signal of the AFA, right side: relative error of the frequency estimation. Each row belongs to a different data loss pattern.

only one sensor was used. This sensor measured a triangle wave generated by a signal generator. The data sent by the sensor were processed on the PC.

As data transmission and acquisition are performed in a hard real-time manner, there is no possibility for re-measurement or re-transmission: data loss is inevitable. Lost data are recognized with a time-out mechanism. To create measurements with different data availability rates, the sensor was placed in a metal cabinet with a sliding door. The data availability was roughly controlled by varying the door position.

Fig. 7 shows the frequency estimate and the error signal of the AFA. The frequency estimate clearly shows the original pattern of changing the frequency from 100 Hz through 150 and 50 Hz and back to 100 Hz in 10 Hz steps. The error signal is approximately zero in most of the time, the Fourier coefficient estimates also converged. During the measurement, data loss occasionally caused the AFA to lose the convergence, but it was always regained quickly.

V. Conclusion

The paper dealt with adaptive Fourier analysis in the case of data loss. After recalling the original RBO and AFA structures, and the mathematical description of the data loss, the handling of data loss has been discussed. First the modified RBO has been presented, then the main innovation of this paper, the modified AFA has been introduced. The proposed structure was tested with simulations and measurements thoroughly. In

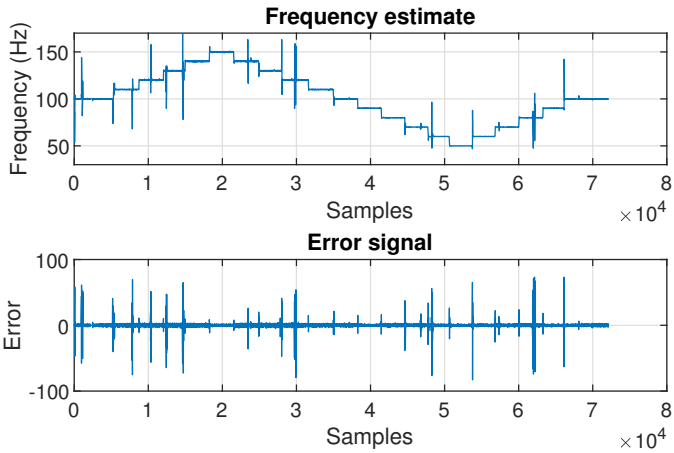

Fig. 7. Estimated frequency and error signal (measurement).

the case of random data loss, the estimates generally converged even when half of the samples were missing. When the data loss is periodic, the data loss tolerance mainly depends on the relation of the periods of the signal and the data loss. Based on the experiences, the modified AFA is able to efficiently determine the harmonic components in the case of data loss.

References

[1] A. Brandt, T. Lagö, K. Ahlin, and J. Tůma, "Main principles and limitations of current order tracking methods," *Sound & vibration*, vol. 39, pp. 19–22, 03 2005.

[2] G. Peceli, "A common structure for recursive discrete transforms," *IEEE Trans. Circuits Syst.*, vol. 33, no. 10, pp. 1035–1036, 1986.

[3] F. Nagy, "Measurement of signal parameters using nonlinear observers," *IEEE Trans. Instrum. Meas.*, vol. 41, no. 1, pp. 152–155, 1992.

[4] L. Sujbert, G. Simon, and G. Peceli, "An observer-based adaptive fourier analysis [tips & tricks]," *IEEE Signal Process. Mag.*, vol. 37, no. 4, pp. 134–143, 2020.

[5] F. Nagy, "An adaptive fourier analysis algorithm," in *5th Int. Conf. on Signal Process. Appl. and Technol.*, Dallas, TX, Oct. 19–22 1994, pp. 414–418.

[6] A. Ronk, "Extended block-adaptive fourier analyser," in *1st IEEE Int. Conf. on Circuits and Systems for Commun. Proc.*, 2002, pp. 428–431.

[7] T. Dabóczi, "Robust adaptive fourier analyzer," in *Int. Conf. on Innovative Technol.*, Budapest, Hungary, Sept. 10–12 2013, pp. 257—-260.

[8] G. Simon and G. Peceli, "Convergence properties of an adaptive fourier analyzer," *IEEE Trans. Circuits Syst. II*, vol. 46, no. 2, pp. 223–227, 1999.

[9] L. Sujbert, G. Simon, and A. Várkonyi-Kóczy, "An improved adaptive fourier analyzer," in *IEEE Int. Workshop on Intell. Signal Process.*, Budapest, Hungary, Sept. 1999, pp. 182–187.

[10] A. R. Varkonyi-Koczy, G. Simon, L. Sujbert, and M. Fek, "A fast filter-bank for adaptive fourier analysis," *IEEE Trans. Instrum. Meas.*, vol. 47, no. 5, pp. 1124–1128, 1998.

[11] C. Hajdu, C. Zamantzas, and T. Daboczi, "A resource-efficient adaptive fourier analyzer," *J. of Instrum.*, vol. 11, P10014, pp. 1–13, 10 2016.

[12] G. Orosz, L. Sujbert, and G. Peceli, "Analysis of resonator-based harmonic estimation in the case of data loss," *IEEE Trans. Instrum. Meas.*, vol. 62, no. 2, pp. 510–518, 2013.

[13] A. Palkó and L. Sujbert, "FFT-based identification of Gilbert-Elliott data loss models," in *2020 IEEE Int. Instrum. and Meas. Technol. Conf. (I2MTC)*, Dubrovnik, Croatia, May 2020, pp. 1–6.

[14] G. Orosz, L. Sujbert, and G. Peceli, "Testbed for wireless adaptive signal processing systems," in *2007 IEEE Instrumentation Measurement Technology Conference IMTC 2007*, 2007, pp. 1–6.